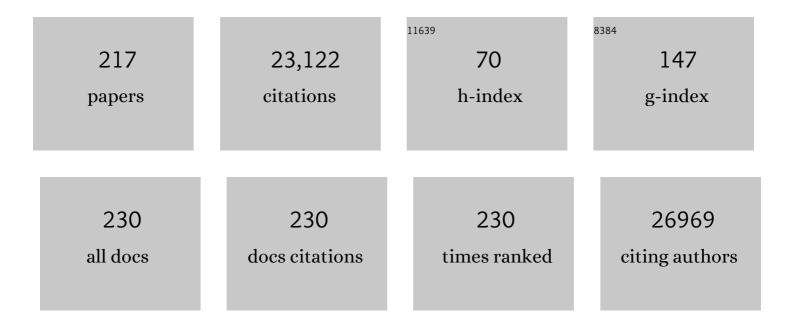
## Sanjiv Sam Gambhir

List of Publications by Year in descending order

Source: https://exaly.com/author-pdf/3693974/publications.pdf

Version: 2024-02-01



#	Article	IF	CITATIONS
1	Molecular imaging of cancer with positron emission tomography. Nature Reviews Cancer, 2002, 2, 683-693.	12.8	1,481
2	Carbon nanotubes as photoacoustic molecular imaging agents in living mice. Nature Nanotechnology, 2008, 3, 557-562.	15.6	1,215
3	Semiconducting polymer nanoparticles as photoacoustic molecular imaging probes in living mice. Nature Nanotechnology, 2014, 9, 233-239.	15.6	1,057
4	A brain tumor molecular imaging strategy using a new triple-modality MRI-photoacoustic-Raman nanoparticle. Nature Medicine, 2012, 18, 829-834.	15.2	1,029
5	Molecular imaging in drug development. Nature Reviews Drug Discovery, 2008, 7, 591-607.	21.5	1,000
6	A Molecular Imaging Primer: Modalities, Imaging Agents, and Applications. Physiological Reviews, 2012, 92, 897-965.	13.1	928
7	Nanomaterials for In Vivo Imaging. Chemical Reviews, 2017, 117, 901-986.	23.0	879
8	Multiplexed imaging of surface enhanced Raman scattering nanotags in living mice using noninvasive Raman spectroscopy. Proceedings of the National Academy of Sciences of the United States of America, 2009, 106, 13511-13516.	3.3	656
9	First-in-human liver-tumour surgery guided by multispectral fluorescence imaging in the visible and near-infrared-I/II windows. Nature Biomedical Engineering, 2020, 4, 259-271.	11.6	622
10	Molecular Imaging with Theranostic Nanoparticles. Accounts of Chemical Research, 2011, 44, 1050-1060.	7.6	464
11	Noninvasive cell-tracking methods. Nature Reviews Clinical Oncology, 2011, 8, 677-688.	12.5	439
12	Integrating genomic features for non-invasive early lung cancer detection. Nature, 2020, 580, 245-251.	13.7	379
13	Photoacoustic clinical imaging. Photoacoustics, 2019, 14, 77-98.	4.4	368
14	Matrix-insensitive protein assays push the limits of biosensors in medicine. Nature Medicine, 2009, 15, 1327-1332.	15.2	359
15	Gold Nanorods for Ovarian Cancer Detection with Photoacoustic Imaging and Resection Guidance <i>via</i> Raman Imaging in Living Mice. ACS Nano, 2012, 6, 10366-10377.	7.3	357
16	Miniature gold nanorods for photoacoustic molecular imaging in the second near-infrared optical window. Nature Nanotechnology, 2019, 14, 465-472.	15.6	349
17	Noninvasive detection of therapeutic cytolytic T cells with 18F–FHBG PET in a patient with glioma. Nature Clinical Practice Oncology, 2009, 6, 53-58.	4.3	345
18	Ex vivo cell labeling with 64Cu-pyruvaldehyde-bis(N4-methylthiosemicarbazone) for imaging cell trafficking in mice with positron-emission tomography. Proceedings of the National Academy of Sciences of the United States of America, 2002, 99, 3030-3035.	3.3	333

#	Article	IF	CITATIONS
19	Engineering high-affinity PD-1 variants for optimized immunotherapy and immuno-PET imaging. Proceedings of the National Academy of Sciences of the United States of America, 2015, 112, E6506-14.	3.3	299
20	Early detection of cancer. Science, 2022, 375, eaay9040.	6.0	291
21	Eradication of spontaneous malignancy by local immunotherapy. Science Translational Medicine, 2018, 10, .	5.8	289
22	The Exosome Total Isolation Chip. ACS Nano, 2017, 11, 10712-10723.	7.3	275
23	Reporter gene imaging of targeted T cell immunotherapy in recurrent glioma. Science Translational Medicine, 2017, 9, .	5.8	263
24	Towards clinically translatable in vivo nanodiagnostics. Nature Reviews Materials, 2017, 2, .	23.3	255
25	A Novel High-Sensitivity Rapid-Acquisition Single-Photon Cardiac Imaging Camera. Journal of Nuclear Medicine, 2009, 50, 635-643.	2.8	241
26	Quantification of target gene expression by imaging reporter gene expression in living animals. Nature Medicine, 2000, 6, 933-937.	15.2	219
27	Selective uptake of single-walled carbon nanotubes by circulating monocytes for enhanced tumour delivery. Nature Nanotechnology, 2014, 9, 481-487.	15.6	216
28	Mathematical Model Identifies Blood Biomarker–Based Early Cancer Detection Strategies and Limitations. Science Translational Medicine, 2011, 3, 109ra116.	5.8	202
29	Activatable Oligomerizable Imaging Agents for Photoacoustic Imaging of Furin-Like Activity in Living Subjects. Journal of the American Chemical Society, 2013, 135, 11015-11022.	6.6	196
30	A small animal Raman instrument for rapid, wide-area, spectroscopic imaging. Proceedings of the National Academy of Sciences of the United States of America, 2013, 110, 12408-12413.	3.3	185
31	Clinically Approved Nanoparticle Imaging Agents. Journal of Nuclear Medicine, 2016, 57, 1833-1837.	2.8	181
32	Tumor Cell-Derived Extracellular Vesicle-Coated Nanocarriers: An Efficient Theranostic Platform for the Cancer-Specific Delivery of Anti-miR-21 and Imaging Agents. ACS Nano, 2018, 12, 10817-10832.	7.3	170
33	Mitochondrial copper depletion suppresses triple-negative breast cancer in mice. Nature Biotechnology, 2021, 39, 357-367.	9.4	163
34	Carbon-coated FeCo nanoparticles as sensitive magnetic-particle-imaging tracers with photothermal and magnetothermal properties. Nature Biomedical Engineering, 2020, 4, 325-334.	11.6	160
35	Pilot Comparison of <sup>68</sup> Ga-RM2 PET and <sup>68</sup> Ga-PSMA-11 PET in Patients with Biochemically Recurrent Prostate Cancer. Journal of Nuclear Medicine, 2016, 57, 557-562.	2.8	155
36	Development and MPI tracking of novel hypoxia-targeted theranostic exosomes. Biomaterials, 2018, 177, 139-148.	5.7	155

#	Article	IF	CITATIONS
37	Molecular Imaging: The Vision and Opportunity for Radiology in the Future. Radiology, 2007, 244, 39-47.	3.6	151
38	The Fate and Toxicity of Raman-Active Silica-Gold Nanoparticles in Mice. Science Translational Medicine, 2011, 3, 79ra33.	5.8	139
39	Novel Radiotracer for ImmunoPET Imaging of PD-1 Checkpoint Expression on Tumor Infiltrating Lymphocytes. Bioconjugate Chemistry, 2015, 26, 2062-2069.	1.8	139
40	Toward achieving precision health. Science Translational Medicine, 2018, 10, .	5.8	134
41	Pilot Pharmacokinetic and Dosimetric Studies of <sup>18</sup> F-FPPRGD2: A PET Radiopharmaceutical Agent for Imaging α <sub>v</sub> β <sub>3</sub> Integrin Levels. Radiology, 2011, 260, 182-191.	3.6	131
42	Endoscopic molecular imaging of human bladder cancer using a CD47 antibody. Science Translational Medicine, 2014, 6, 260ra148.	5.8	124
43	PET imaging of herpes simplex virus type 1 thymidine kinase (HSV1-tk) or mutant HSV1-sr39tk reporter gene expression in mice and humans using [18F]FHBC. Nature Protocols, 2006, 1, 3069-3074.	5.5	118
44	Exploratory Clinical Trial of (4 <i>S</i> )-4-(3-[18F]fluoropropyl)- <scp> </scp> -glutamate for Imaging xCâ^ Transporter Using Positron Emission Tomography in Patients with Non–Small Cell Lung or Breast Cancer. Clinical Cancer Research, 2012, 18, 5427-5437.	3.2	114
45	Imaging activated T cells predicts response to cancer vaccines. Journal of Clinical Investigation, 2018, 128, 2569-2580.	3.9	114
46	A mountable toilet system for personalized health monitoring via the analysis of excreta. Nature Biomedical Engineering, 2020, 4, 624-635.	11.6	112
47	Imaging progress of herpes simplex virus type 1 thymidine kinase suicide gene therapy in living subjects with positron emission tomography. Cancer Gene Therapy, 2005, 12, 329-339.	2.2	107
48	Tomographic magnetic particle imaging of cancer targeted nanoparticles. Nanoscale, 2017, 9, 18723-18730.	2.8	107
49	A Real-Time Clinical Endoscopic System for Intraluminal, Multiplexed Imaging of Surface-Enhanced Raman Scattering Nanoparticles. PLoS ONE, 2015, 10, e0123185.	1.1	106
50	A mathematical model of ctDNA shedding predicts tumor detection size. Science Advances, 2020, 6, .	4.7	105
51	Seeing is believing: Non-invasive, quantitative and repetitive imaging of reporter gene expression in living animals, using positron emission tomography. Journal of Neuroscience Research, 2000, 59, 699-705.	1.3	103
52	Practical Immuno-PET Radiotracer Design Considerations for Human Immune Checkpoint Imaging. Journal of Nuclear Medicine, 2017, 58, 538-546.	2.8	102
53	Engineered immune cells as highly sensitive cancer diagnostics. Nature Biotechnology, 2019, 37, 531-539.	9.4	101
54	A PET Imaging Strategy to Visualize Activated T Cells in Acute Graft-versus-Host Disease Elicited by Allogenic Hematopoietic Cell Transplant. Cancer Research, 2017, 77, 2893-2902.	0.4	98

#	Article	IF	CITATIONS
55	Prospective Comparison of <sup>99m</sup> Tc-MDP Scintigraphy, Combined <sup>18</sup> F-NaF and <sup>18</sup> F-FDG PET/CT, and Whole-Body MRI in Patients with Breast and Prostate Cancer. Journal of Nuclear Medicine, 2015, 56, 1862-1868.	2.8	95
56	Comparison of [ 18 F]FHBG and [ 14 C]FIAU for imaging of HSV1-tk reporter gene expression: adenoviral infection vs stable transfection. European Journal of Nuclear Medicine and Molecular Imaging, 2003, 30, 1547-1560.	3.3	94
57	Imaging approaches to optimize molecular therapies. Science Translational Medicine, 2016, 8, 355ps16.	5.8	93
58	An intravascular magnetic wire for the high-throughput retrieval of circulating tumour cells in vivo. Nature Biomedical Engineering, 2018, 2, 696-705.	11.6	92
59	Development of Novel ImmunoPET Tracers to Image Human PD-1 Checkpoint Expression on Tumor-Infiltrating Lymphocytes in a Humanized Mouse Model. Molecular Imaging and Biology, 2017, 19, 903-914.	1.3	91
60	Molecular profiling of single circulating tumor cells from lung cancer patients. Proceedings of the National Academy of Sciences of the United States of America, 2016, 113, E8379-E8386.	3.3	90
61	Simultaneous transrectal ultrasound and photoacoustic human prostate imaging. Science Translational Medicine, 2019, 11, .	5.8	87
62	Trop2 is a driver of metastatic prostate cancer with neuroendocrine phenotype via PARP1. Proceedings of the National Academy of Sciences of the United States of America, 2020, 117, 2032-2042.	3.3	85
63	Investigation of 6-[18F]-Fluoromaltose as a Novel PET Tracer for Imaging Bacterial Infection. PLoS ONE, 2014, 9, e107951.	1.1	85
64	New Positron Emission Tomography (PET) Radioligand for Imaging σ-1 Receptors in Living Subjects. Journal of Medicinal Chemistry, 2012, 55, 8272-8282.	2.9	81
65	Surface-Enhanced Raman Scattering Nanoparticles for Multiplexed Imaging of Bladder Cancer Tissue Permeability and Molecular Phenotype. ACS Nano, 2018, 12, 9669-9679.	7.3	81
66	Fluorescent Magnetic Nanoparticles for Magnetically Enhanced Cancer Imaging and Targeting in Living Subjects. ACS Nano, 2012, 6, 6862-6869.	7.3	79
67	Specific Imaging of Bacterial Infection Using 6″- <sup>18</sup> F-Fluoromaltotriose: A Second-Generation PET Tracer Targeting the Maltodextrin Transporter in Bacteria. Journal of Nuclear Medicine, 2017, 58, 1679-1684.	2.8	79
68	Maltotriose-based probes for fluorescence and photoacoustic imaging of bacterial infections. Nature Communications, 2020, 11, 1250.	5.8	78
69	Deep Tissue Photoacoustic Imaging Using a Miniaturized 2-D Capacitive Micromachined Ultrasonic Transducer Array. IEEE Transactions on Biomedical Engineering, 2012, 59, 1199-1204.	2.5	73
70	ICOS Is an Indicator of T-cell–Mediated Response to Cancer Immunotherapy. Cancer Research, 2020, 80, 3023-3032.	0.4	72
71	Multiparametric Photoacoustic Analysis of Human Thyroid Cancers <i>In Vivo</i> . Cancer Research, 2021, 81, 4849-4860.	0.4	72
72	Simultaneous Whole-Body Time-of-Flight 18F-FDG PET/MRI. Clinical Nuclear Medicine, 2015, 40, 1-8.	0.7	70

#	Article	IF	CITATIONS
73	Proof-of-Concept Study of Monitoring Cancer Drug Therapy with Cerenkov Luminescence Imaging. Journal of Nuclear Medicine, 2012, 53, 312-317.	2.8	68
74	The Immunoimaging Toolbox. Journal of Nuclear Medicine, 2018, 59, 1174-1182.	2.8	68
75	A PET imaging approach for determining EGFR mutation status for improved lung cancer patient management. Science Translational Medicine, 2018, 10, .	5.8	66
76	Gene therapy imaging in patients for oncological applications. European Journal of Nuclear Medicine and Molecular Imaging, 2005, 32, S384-S403.	3.3	61
77	Circulating Tumor Microemboli Diagnostics for Patients with Non–Small-Cell Lung Cancer. Journal of Thoracic Oncology, 2014, 9, 1111-1119.	0.5	61
78	Emerging Intraoperative Imaging Modalities to Improve Surgical Precision. Molecular Imaging and Biology, 2018, 20, 705-715.	1.3	61
79	Low-frequency ultrasound-mediated cytokine transfection enhances T cell recruitment at local and distant tumor sites. Proceedings of the National Academy of Sciences of the United States of America, 2020, 117, 12674-12685.	3.3	61
80	Comparison of [14C]FMAU, [3H]FEAU, [14C]FIAU, and [3H]PCV for Monitoring Reporter Gene Expression of Wild Type and Mutant Herpes Simplex Virus Type 1 Thymidine Kinase in Cell Culture. Molecular Imaging and Biology, 2005, 7, 296-303.	1.3	59
81	Evaluation of a <sup>64</sup> Cu-Labeled Cystine-Knot Peptide Based on Agouti-Related Protein for PET of Tumors Expressing α <sub>v</sub> î² <sub>3</sub> Integrin. Journal of Nuclear Medicine, 2010, 51, 251-258.	2.8	59
82	High-sensitivity, real-time, ratiometric imaging of surface-enhanced Raman scattering nanoparticles with a clinically translatable Raman endoscope device. Journal of Biomedical Optics, 2013, 18, 1.	1.4	58
83	Plasmonic and Electrostatic Interactions Enable Uniformly Enhanced Liquid Bacterial Surface-Enhanced Raman Scattering (SERS). Nano Letters, 2020, 20, 7655-7661.	4.5	56
84	PET imaging of tumor glycolysis downstream of hexokinase through noninvasive measurement of pyruvate kinase M2. Science Translational Medicine, 2015, 7, 310ra169.	5.8	54
85	Microvesicle-Mediated Delivery of Minicircle DNA Results in Effective Gene-Directed Enzyme Prodrug Cancer Therapy. Molecular Cancer Therapeutics, 2019, 18, 2331-2342.	1.9	54
86	Molecular Imaging of Chimeric Antigen Receptor T Cells by ICOS-ImmunoPET. Clinical Cancer Research, 2021, 27, 1058-1068.	3.2	53
87	Reconstructed Apoptotic Bodies as Targeted "Nano Decoys―to Treat Intracellular Bacterial Infections within Macrophages and Cancer Cells. ACS Nano, 2020, 14, 5818-5835.	7.3	52
88	Pilot Preclinical and Clinical Evaluation of (4S)-4-(3-[18F]Fluoropropyl)-L-Glutamate (18F-FSPG) for PET/CT Imaging of Intracranial Malignancies. PLoS ONE, 2016, 11, e0148628.	1.1	51
89	Glioblastoma Multiforme Recurrence: An Exploratory Study of18F FPPRGD2PET/CT. Radiology, 2015, 277, 497-506.	3.6	49
90	A Systematic Comparison of 18F-C-SNAT to Established Radiotracer Imaging Agents for the Detection of Tumor Response to Treatment. Clinical Cancer Research, 2015, 21, 3896-3905.	3.2	48

#	Article	IF	CITATIONS
91	Initial experience with a SiPM-based PET/CT scanner: influence of acquisition time on image quality. EJNMMI Physics, 2018, 5, 9.	1.3	47
92	Molecular Imaging of PET Reporter Gene Expression. Handbook of Experimental Pharmacology, 2008, , 277-303.	0.9	46
93	Detecting cancers through tumor-activatable minicircles that lead to a detectable blood biomarker. Proceedings of the National Academy of Sciences of the United States of America, 2015, 112, 3068-3073.	3.3	46
94	Whole-body tracking of single cells via positron emission tomography. Nature Biomedical Engineering, 2020, 4, 835-844.	11.6	46
95	A strategy for blood biomarker amplification and localization using ultrasound. Proceedings of the National Academy of Sciences of the United States of America, 2009, 106, 17152-17157.	3.3	43
96	Biodistribution of the 18F-FPPRGD2 PET radiopharmaceutical in cancer patients: an atlas of SUV measurements. European Journal of Nuclear Medicine and Molecular Imaging, 2015, 42, 1850-1858.	3.3	43
97	18F-FDG silicon photomultiplier PET/CT: A pilot study comparing semi-quantitative measurements with standard PET/CT. PLoS ONE, 2017, 12, e0178936.	1.1	43
98	A Comparison Between a Time Domain and Continuous Wave Small Animal Optical Imaging System. IEEE Transactions on Medical Imaging, 2008, 27, 58-63.	5.4	42
99	Assessment of Tumor Redox Status through ( <i>S</i> )-4-(3-[18F]fluoropropyl)- <scp>L</scp> -Glutamic Acid PET Imaging of System xcâ^² Activity. Cancer Research, 2022, 79, 853-863.	0.4	42
100	Reduction Triggered <i>In Situ</i> Polymerization in Living Mice. Journal of the American Chemical Society, 2020, 142, 15575-15584.	6.6	42
101	Nanomedicine for Spontaneous Brain Tumors: A Companion Clinical Trial. ACS Nano, 2019, 13, 2858-2869.	7.3	41
102	Detection of Premalignant Gastrointestinal Lesions Using Surface-Enhanced Resonance Raman Scattering–Nanoparticle Endoscopy. ACS Nano, 2019, 13, 1354-1364.	7.3	40
103	A High-Affinity, High-Stability Photoacoustic Agent for Imaging Gastrin-Releasing Peptide Receptor in Prostate Cancer. Clinical Cancer Research, 2014, 20, 3721-3729.	3.2	39
104	Continuous health monitoring: An opportunity for precision health. Science Translational Medicine, 2021, 13, .	5.8	39
105	The Project Baseline Health Study: a step towards a broader mission to map human health. Npj Digital Medicine, 2020, 3, 84.	5.7	38
106	A protease-activated, near-infrared fluorescent probe for early endoscopic detection of premalignant gastrointestinal lesions. Proceedings of the National Academy of Sciences of the United States of America, 2021, 118, .	3.3	38
107	<sup>64</sup> Cu-Labeled Divalent Cystine Knot Peptide for Imaging Carotid Atherosclerotic Plaques. Journal of Nuclear Medicine, 2015, 56, 939-944.	2.8	36
108	Imaging B Cells in a Mouse Model of Multiple Sclerosis Using <sup>64</sup> Cu-Rituximab PET. Journal of Nuclear Medicine, 2017, 58, 1845-1851.	2.8	35

#	Article	IF	CITATIONS
109	A Novel Theranostic Strategy for <i>MMP-14</i> –Expressing Glioblastomas Impacts Survival. Molecular Cancer Therapeutics, 2017, 16, 1909-1921.	1.9	35
110	AshwaMAX and Withaferin A inhibits gliomas in cellular and murine orthotopic models. Journal of Neuro-Oncology, 2016, 126, 253-264.	1.4	34
111	Biodistribution and Radiation Dosimetry of <sup>18</sup> F-FTC-146 in Humans. Journal of Nuclear Medicine, 2017, 58, 2004-2009.	2.8	34
112	Imaging Circulating Tumor Cells in Freely Moving Awake Small Animals Using a Miniaturized Intravital Microscope. PLoS ONE, 2014, 9, e86759.	1.1	33
113	Introduction: FIGURE 1 Journal of Nuclear Medicine, 2008, 49, 1S-4S.	2.8	32
114	A Model-Based Personalized Cancer Screening Strategy for Detecting Early-Stage Tumors Using Blood-Borne Biomarkers. Cancer Research, 2017, 77, 2570-2584.	0.4	32
115	Synthesis of [18F]-labelled Maltose Derivatives as PET Tracers for Imaging Bacterial Infection. Molecular Imaging and Biology, 2015, 17, 168-176.	1.3	31
116	Positron emission tomography reporter gene strategy for use in the central nervous system. Proceedings of the National Academy of Sciences of the United States of America, 2019, 116, 11402-11407.	3.3	31
117	Positron Emission Tomography of 64Cu-DOTA-Rituximab in a Transgenic Mouse Model Expressing Human CD20 for Clinical Translation to Image NHL. Molecular Imaging and Biology, 2012, 14, 608-616.	1.3	30
118	Deactivated CRISPR Associated Protein 9 for Minor-Allele Enrichment in Cell-Free DNA. Clinical Chemistry, 2018, 64, 307-316.	1.5	30
119	A Novel Engineered Small Protein for Positron Emission Tomography Imaging of Human Programmed Death Ligand-1: Validation in Mouse Models and Human Cancer Tissues. Clinical Cancer Research, 2019, 25, 1774-1785.	3.2	30
120	A photonic crystal cavity-optical fiber tip nanoparticle sensor for biomedical applications. Applied Physics Letters, 2012, 100, .	1.5	29
121	Synthesis of (4-[18F]fluorophenyl)triphenylphosphonium as a potential imaging agent for mitochondrial dysfunction. Journal of Labelled Compounds and Radiopharmaceuticals, 2005, 48, 131-137.	0.5	28
122	Biodegradable Fluorescent Nanoparticles for Endoscopic Detection of Colorectal Carcinogenesis. Advanced Functional Materials, 2019, 29, 1904992.	7.8	28
123	A Clinical Wide-Field Fluorescence Endoscopic Device for Molecular Imaging Demonstrating Cathepsin Protease Activity in Colon Cancer. Molecular Imaging and Biology, 2016, 18, 820-829.	1.3	27
124	SP94-Targeted Triblock Copolymer Nanoparticle Delivers Thymidine Kinase–p53–Nitroreductase Triple Therapeutic Gene and Restores Anticancer Function against Hepatocellular Carcinoma in Vivo. ACS Applied Materials & Interfaces, 2020, 12, 11307-11319.	4.0	27
125	Superiorized Photo-Acoustic Non-NEgative Reconstruction (SPANNER) for Clinical Photoacoustic Imaging. IEEE Transactions on Medical Imaging, 2021, 40, 1888-1897.	5.4	26
126	Improving Image Quality by Accounting for Changes in Water Temperature during a Photoacoustic Tomography Scan. PLoS ONE, 2012, 7, e45337.	1.1	25

#	Article	IF	CITATIONS
127	Pilot prospective evaluation of 18F-FPPRGD2 PET/CT in patients with cervical and ovarian cancer. European Journal of Nuclear Medicine and Molecular Imaging, 2016, 43, 1047-1055.	3.3	25
128	Synergistic inhibition of glioma cell proliferation by Withaferin A and tumor treating fields. Journal of Neuro-Oncology, 2017, 134, 259-268.	1.4	25
129	PET Imaging of TIGIT Expression on Tumor-Infiltrating Lymphocytes. Clinical Cancer Research, 2021, 27, 1932-1940.	3.2	25
130	Detection of Stem Cell Transplant Rejection with Ferumoxytol MR Imaging: Correlation of MR Imaging Findings with Those at Intravital Microscopy. Radiology, 2017, 284, 495-507.	3.6	24
131	PET Reporter Gene Imaging and Ganciclovir-Mediated Ablation of Chimeric Antigen Receptor T Cells in Solid Tumors. Cancer Research, 2020, 80, 4731-4740.	0.4	24
132	Ultraselective Carbon Nanotubes for Photoacoustic Imaging of Inflamed Atherosclerotic Plaques. Advanced Functional Materials, 2021, 31, 2101005.	7.8	24
133	A Cystine Knot Peptide Targeting Integrin α <sub>v</sub> β <sub>6</sub> for Photoacoustic and Fluorescence Imaging of Tumors in Living Subjects. Journal of Nuclear Medicine, 2016, 57, 1629-1634.	2.8	22
134	[18F]FSPG-PET reveals increased cystine/glutamate antiporter (xc-) activity in a mouse model of multiple sclerosis. Journal of Neuroinflammation, 2018, 15, 55.	3.1	21
135	Visualization of Activated T Cells by OX40-ImmunoPET as a Strategy for Diagnosis of Acute Graft-versus-Host Disease. Cancer Research, 2020, 80, 4780-4790.	0.4	21
136	Development and Validation of Non-Integrative, Self-Limited, and Replicating Minicircles for Safe Reporter Gene Imaging of Cell-Based Therapies. PLoS ONE, 2013, 8, e73138.	1.1	21
137	Isolation and Characterization of a Monobody with a Fibronectin Domain III Scaffold That Specifically Binds EphA2. PLoS ONE, 2015, 10, e0132976.	1.1	20
138	Development and Validation of an Immuno-PET Tracer as a Companion Diagnostic Agent for Antibody-Drug Conjugate Therapy to Target the CA6 Epitope. Radiology, 2015, 276, 191-198.	3.6	20
139	Discovery and Optimization of Small-Molecule Ligands for V-Domain Ig Suppressor of T-Cell Activation (VISTA). Journal of the American Chemical Society, 2020, 142, 16194-16198.	6.6	19
140	Noninvasive and Highly Multiplexed Five-Color Tumor Imaging of Multicore Near-Infrared Resonant Surface-Enhanced Raman Nanoparticles <i>In Vivo</i> . ACS Nano, 2021, 15, 19956-19969.	7.3	19
141	Improved detection of prostate cancer using a magneto-nanosensor assay for serum circulating autoantibodies. PLoS ONE, 2019, 14, e0221051.	1.1	18
142	Molecular Imaging of Biological Gene Delivery Vehicles for Targeted Cancer Therapy: Beyond Viral Vectors. Nuclear Medicine and Molecular Imaging, 2010, 44, 15-24.	0.6	17
143	Development of [18F]DASA-23 for Imaging Tumor Glycolysis Through Noninvasive Measurement of Pyruvate Kinase M2. Molecular Imaging and Biology, 2017, 19, 665-672.	1.3	16
144	A Magnetic Bead-Based Sensor for the Quantification of Multiple Prostate Cancer Biomarkers. PLoS ONE, 2015, 10, e0139484.	1.1	15

#	Article	IF	CITATIONS
145	Semiquantitative Analysis of the Biodistribution of the Combined 18F-NaF and 18F-FDG Administration for PET/CT Imaging. Journal of Nuclear Medicine, 2015, 56, 688-694.	2.8	15
146	Characterization of Physiologic <sup>18</sup> F FSPG Uptake in Healthy Volunteers. Radiology, 2016, 279, 898-905.	3.6	15
147	Clinical Evaluation of (4S)-4-(3-[18F]Fluoropropyl)-L-glutamate (18F-FSPG) for PET/CT Imaging in Patients with Newly Diagnosed and Recurrent Prostate Cancer. Clinical Cancer Research, 2020, 26, 5380-5387.	3.2	15
148	Ultra-high-frequency radio-frequency acoustic molecular imaging with saline nanodroplets in living subjects. Nature Nanotechnology, 2021, 16, 717-724.	15.6	15
149	Multiparameter Longitudinal Imaging of Immune Cell Activity in Chimeric Antigen Receptor T Cell and Checkpoint Blockade Therapies. ACS Central Science, 2022, 8, 590-602.	5.3	15
150	Giant Magnetoresistive Nanosensor Analysis of Circulating Tumor DNA Epidermal Growth Factor Receptor Mutations for Diagnosis and Therapy Response Monitoring. Clinical Chemistry, 2021, 67, 534-542.	1.5	14
151	Alk5 inhibition increases delivery of macromolecular and protein-bound contrast agents to tumors. JCI Insight, 2016, 1, .	2.3	13
152	Longitudinal Monitoring of Antibody Responses against Tumor Cells Using Magneto-nanosensors with a Nanoliter of Blood. Nano Letters, 2017, 17, 6644-6652.	4.5	13
153	Evaluation of Glycolytic Response to Multiple Classes of Anti-glioblastoma Drugs by Noninvasive Measurement of Pyruvate Kinase M2 Using [18F]DASA-23. Molecular Imaging and Biology, 2020, 22, 124-133.	1.3	13
154	Tumor treating fields (TTFields) impairs aberrant glycolysis in glioblastoma as evaluated by [18F]DASA-23, a non-invasive probe of pyruvate kinase M2 (PKM2) expression. Neoplasia, 2021, 23, 58-67.	2.3	13
155	Detection and Quantitation of Circulating Tumor Cell Dynamics by Bioluminescence Imaging in an Orthotopic Mammary Carcinoma Model. PLoS ONE, 2014, 9, e105079.	1.1	13
156	Tumor characterization by ultrasound-release of multiple protein and microRNA biomarkers, preclinical and clinical evidence. PLoS ONE, 2018, 13, e0194268.	1.1	12
157	The Utility of [18F]DASA-23 for Molecular Imaging of Prostate Cancer with Positron Emission Tomography. Molecular Imaging and Biology, 2018, 20, 1015-1024.	1.3	11
158	[18F]-SuPAR: A Radiofluorinated Probe for Noninvasive Imaging of DNA Damage-Dependent Poly(ADP-ribose) Polymerase Activity. Bioconjugate Chemistry, 2019, 30, 1331-1342.	1.8	11
159	A novel synthesis of 6′′â€{ <sup>18</sup> F]â€fluoromaltotriose as a PET tracer for imaging bacterial infection. Journal of Labelled Compounds and Radiopharmaceuticals, 2018, 61, 408-414.	0.5	10
160	The Characterization of 18F-hGTS13 for Molecular Imaging of xCâ^' Transporter Activity with PET. Journal of Nuclear Medicine, 2019, 60, 1812-1817.	2.8	10
161	Human biodistribution and radiation dosimetry of [18F]DASA-23, a PET probe targeting pyruvate kinase M2. European Journal of Nuclear Medicine and Molecular Imaging, 2020, 47, 2123-2130.	3.3	10
162	Return of individual research results: What do participants prefer and expect?. PLoS ONE, 2021, 16, e0254153.	1.1	10

#	Article	IF	CITATIONS
163	Whole-body PET Imaging of T-cell Response to Glioblastoma. Clinical Cancer Research, 2021, 27, 6445-6456.	3.2	10
164	Pilot-phase PET/CT study targeting integrin αvβ6 in pancreatic cancer patients using the cystine-knot peptide–based 18F-FP-R01-MG-F2. European Journal of Nuclear Medicine and Molecular Imaging, 2021, , 1.	3.3	10
165	Molecular Imaging of Infective Endocarditis With 6′′-[ <sup>18</sup> F]Fluoromaltotriose Positron Emission Tomography–Computed Tomography. Circulation, 2020, 141, 1729-1731.	1.6	9
166	A Clinical PET Imaging Tracer ([18F]DASA-23) to Monitor Pyruvate Kinase M2–Induced Glycolytic Reprogramming in Glioblastoma. Clinical Cancer Research, 2021, 27, 6467-6478.	3.2	9
167	Ferumoxytol-based Dual-modality Imaging Probe for Detection of Stem Cell Transplant Rejection. Nanotheranostics, 2018, 2, 306-319.	2.7	8
168	A Dual-Modality Hybrid Imaging System Harnesses Radioluminescence and Sound to Reveal Molecular Pathology of Atherosclerotic Plaques. Scientific Reports, 2018, 8, 8992.	1.6	8
169	Design and evaluation of Raman reporters for the Raman-silent region. Nanotheranostics, 2022, 6, 1-9.	2.7	8
170	Artificial MicroRNAs as Novel Secreted Reporters for Cell Monitoring in Living Subjects. PLoS ONE, 2016, 11, e0159369.	1.1	7
171	New synthesis of 6″â€{ <sup>18</sup> F]fluoromaltotriose for positron emission tomography imaging of bacterial infection. Journal of Labelled Compounds and Radiopharmaceuticals, 2020, 63, 466-475.	0.5	7
172	Non-Invasive Photoacoustic Imaging of In Vivo Mice with Erythrocyte Derived Optical Nanoparticles to Detect CAD/MI. Scientific Reports, 2020, 10, 5983.	1.6	7
173	SPECT/CT Imaging, Biodistribution and Radiation Dosimetry of a 177Lu-DOTA-Integrin αvβ6 Cystine Knot Peptide in a Pancreatic Cancer Xenograft Model. Frontiers in Oncology, 2021, 11, 684713.	1.3	7
174	<sup>18</sup> F-FSPG PET/CT Imaging of System x <sub>C</sub> <sup>–</sup> Transporter Activity in Patients with Primary and Metastatic Brain Tumors. Radiology, 2022, 303, 620-631.	3.6	7
175	A comparison of noise models in a hybrid reference spectrum and principal components analysis algorithm for Raman spectroscopy. Journal of Raman Spectroscopy, 2013, 44, 841-856.	1.2	6
176	Quantification of Cerenkov Luminescence Imaging (CLI) Comparable With 3-D PET Standard Measurements. Molecular Imaging, 2018, 17, 153601211878863.	0.7	6
177	Minicircles for a two-step blood biomarker and PET imaging early cancer detection strategy. Journal of Controlled Release, 2021, 335, 281-289.	4.8	6
178	Validation of 64Cu-DOTA-rituximab injection preparation under good manufacturing practices: a PET tracer for imaging of B-cell non-Hodgkin lymphoma. Molecular Imaging, 2015, 14, .	0.7	6
179	How to Prevent a Leaky Pipeline in Academic Radiology: Insights From a FacultyÂSurvey. Journal of the American College of Radiology, 2019, 16, 1220-1224.	0.9	5
180	Synthesis and Characterization of 9-(4-[18F]Fluoro-3-(hydroxymethyl)butyl)-2-(phenylthio)-6-oxopurine as a Novel PET Agent for Mutant Herpes Simplex Virus Type 1 Thymidine Kinase Reporter Gene Imaging. Molecular Imaging and Biology, 2020, 22, 1151-1160.	1.3	5

#	Article	IF	CITATIONS
181	Imaging studies for evaluating gene therapy in translational research. Drug Discovery Today: Technologies, 2005, 2, 335-343.	4.0	4
182	Fluorescent Reporter Proteins. , 2010, , 3-40.		4
183	Bioluminescent Monitoring of NIS-Mediated 131 I Ablative Effects in MCF-7 Xenografts. Molecular Imaging, 2006, 5, 7290.2006.00008.	0.7	4
184	Monitoring Gene Therapy by Positron Emission Tomography. , 2003, , 659-685.		3
185	A blood biomarker for monitoring response to anti-EGFR therapy. Cancer Biomarkers, 2018, 22, 333-344.	0.8	3
186	Two Patient Studies of a Companion Diagnostic Immuno-Positron Emission Tomography (PET) Tracer for Measuring Human CA6 Expression in Cancer for Antibody Drug Conjugate (ADC) Therapy. Molecular Imaging, 2020, 19, 153601212093939.	0.7	3
187	Imaging alloreactive T cells provides early warning of organ transplant rejection. JCI Insight, 2021, 6, .	2.3	3
188	Seeing is believing: Non-invasive, quantitative and repetitive imaging of reporter gene expression in living animals, using positron emission tomography. Journal of Neuroscience Research, 2000, 59, 699.	1.3	3
189	Molecular Imaging of Chimeric Antigen Receptor T Cells By ICOS-Immunopet. Blood, 2020, 136, 5-6.	0.6	3
190	Can multispectral optoacoustic tomography replace sentinel lymph biopsy in melanoma?. Annals of Translational Medicine, 2016, 4, 517-517.	0.7	3
191	Multimodality Imaging of Reporter Genes. , 0, , 113-126.		2
192	Cell-Specific Imaging of Reporter Gene Expression Using a Two-Step Transcriptional Amplification Strategy. , 0, , 127-148.		2
193	Reporter Gene Imaging with PET/SPECT. , 0, , 70-87.		2
194	Imaging patients with breast and prostate cancers using combined 18F NaF/18F FDG and TOF simultaneous PET/ MRI. EJNMMI Physics, 2015, 2, A65.	1.3	2
195	In Vivo Translation of the CIRPI System: Revealing Molecular Pathology of Rabbit Aortic Atherosclerotic Plaques. Journal of Nuclear Medicine, 2019, 60, 1308-1316.	2.8	2
196	Isotopically Encoded Nanotags for Multiplexed Ion Beam Imaging. Advanced Materials Technologies, 2020, 5, 2000098.	3.0	2
197	Ultraselective Carbon Nanotubes for Photoacoustic Imaging of Inflamed Atherosclerotic Plaques (Adv. Funct. Mater. 37/2021). Advanced Functional Materials, 2021, 31, 2170271.	7.8	2
198	Cancer Detection Using an Artificial Secretable MicroRNA Found in Blood and Urine. Biomedicines, 2022, 10, 621.	1.4	2

#	Article	IF	CITATIONS
199	Noninvasive Imaging of Gene Expression with Magnetic Resonance Imaging and Magnetic Resonance Spectroscopy. , 0, , 88-110.		1
200	Clinical Applications of Reporter Gene Technology. , 0, , 297-314.		1
201	Gene Therapy and Imaging of Transgene Expression in Living Subjects. , 0, , 227-238.		1
202	Initial experience with a PET/computed tomography system using silicon photomultiplier detectors. Nuclear Medicine Communications, 2019, 40, 1174-1178.	0.5	1
203	Nuclear Imaging of Endogenous Markers of Lymphocyte Response. , 2022, , 15-59.		1
204	Alternative medicine: therapeutic effects on gastric original signet ring carcinoma via ascorbate and combination with sodium alpha lipoate. BMC Complementary Medicine and Therapies, 2022, 22, 58.	1.2	1
205	In Memoriam—Tandra R. Chaudhuri, Ph.D. (1947–2006). Molecular Imaging and Biology, 2007, 9, 59-59.	1.3	0
206	Quantum dots: Dynamic Visualization of RGD-Quantum Dot Binding to Tumor Neovasculature and Extravasation in Multiple Living Mouse Models Using Intravital Microscopy (Small 20/2010). Small, 2010, 6, n/a-n/a.	5.2	0
207	Imaging Cell Trafficking and Immune Cell Activation Using PET Reporter Genes. , 0, , 258-274.		0
208	Physics, Instrumentation, and Methods for Imaging Reporter Gene Expression in Living Subjects. , 0, , 151-192.		0
209	Reporter Gene Imaging of Cell Signal Transduction. , 0, , 195-226.		0
210	Imaging Regulation of Endogenous Gene Expression in Living Subjects. , 0, , 239-257.		0
211	Imaging of Reporter Genes and Stem Cells. , 0, , 275-296.		0
212	Revealing Biomolecular Mechanisms Through In Vivo Bioluminescence Imaging. , 0, , 41-69.		0
213	Reply: 6″-18F-Fluoromaltotriose PET Evaluation in Escherichia Coli–Induced Myositis: Is There Uptake Saturation in Control?. Journal of Nuclear Medicine, 2018, 59, 1166.2-1167.	2.8	0
214	Molecular Imaging Using Raman Scattering. , 2021, , 343-357.		0
215	Detection of Carotid Artery Stenosis with Intraplaque Hemorrhage and Neovascularization Using a Scanning Interferometer. Nano Letters, 2021, 21, 5714-5721.	4.5	0
216	An approach for optimizing gold nanoparticles for possible medical applications, using correlative electron energy loss and Raman spectroscopies on electron beam lithographically fabricated arrays. Journal of Materials Research, 2021, 36, 3383.	1.2	0

#	Article	IF	CITATIONS
217	Tracking T Cell Activation By OX40 Immuno-PET: A Novel Strategy for Imaging of Graft Versus Host Disease. Blood, 2018, 132, 4527-4527.	0.6	0